Journal of Neuroendocrinology

Journal of Neuroendocrinology, 2016, **28**, 10.1111/jne.12349

© 2015 British Society for Neuroendocrinology

ORIGINAL ARTICLE

Des-Acyl Ghrelin Directly Targets the Arcuate Nucleus in a Ghrelin-Receptor Independent Manner and Impairs the Orexigenic Effect of Ghrelin

G. Fernandez, A. Cabral, M. P. Cornejo, P. N. De Francesco, G. Garcia-Romero, M. Reynaldo and M. Perello

Laboratory of Neurophysiology of the Multidisciplinary Institute of Cell Biology, [IMBICE dependent on the Argentine Research Council (CONICET) and Scientific Research Commission, Province of Buenos Aires (CIC-PBA)], La Plata, Buenos Aires, Argentina.

Journal of Neuroendocrinology

Correspondence to: Dr. Mario Perelló, Calle 526 S/N entre 10 y 11-PO Box 403, La Plata, Buenos Aires 1900, Argentina (e-mail: mperello@imbice.gov.ar)

Ghrelin is a stomach-derived octanoylated peptide hormone that plays a variety of well-established biological roles acting via its specific receptor known as growth hormone secretagogue receptor (GHSR). In plasma, a des-octanoylated form of ghrelin, named des-acyl ghrelin (DAG), also exists. DAG is suggested to be a signalling molecule that has specific targets, including the brain, and regulates some physiological functions. However, no specific receptor for DAG has been reported until now, and, consequently, the potential role of DAG as a hormone has remained a matter of debate. In the present study, we show that DAG specifically binds to and acts on a subset of arcuate nucleus (ARC) cells in a GHSR-independent manner. ARC cells labelled by a DAG fluorescent tracer include the neuropeptide Y (NPY) and non-NPY neurones. Given the well-established role of the ARC in appetite regulation, we tested the effect of centrally administered DAG on food intake. We found that DAG failed to affect dark phase feeding, as well as food intake, after a starvation period; however, it impaired the orexigenic actions of peripherally administered ghrelin. Thus, we conclude that DAG directly targets ARC neurones and antagonises the orexigenic effects of peripherally administered ghrelin.

Key words: des-acyl ghrelin receptor, hypothalamus, acyl-ghrelin, food intake

doi: 10.1111/jne.12349

The ghrelin cells located within the gastric oxyntic mucosa produce at least two peptides, ghrelin and des-acyl ghrelin (DAG), which share the same amino acid sequence but differ with respect to the presence of an octanoyl group at the serine 3 residue (1,2). The acylation of ghrelin occurs in the endoplasmic reticulum of these cells and is catalysed by the enzyme ghrelin O-acyltransferase (GOAT) (1). In plasma, DAG constitutes the majority of total circulating ghrelin immunoreactivity because not only is DAG secreted from the gastrointestinal tract, but also it is produced after rapid deacylation of ghrelin in the circulation (3). For example, the ghrelin : DAG ratio in mice goes from approximately 2.5 in stomach extracts to approximately 0.4 in plasma (4). Current knowledge of the biology of DAG and ghrelin differs significantly. It is well established that ghrelin acts via its specific receptor named the growth hormone secretagogue receptor (GHSR) (5). GHSR is highly expressed in the brain, where ghrelin plays well defined roles in the regulation of growth hormone secretion, food intake, energy expenditure, glucose homeostasis, anxiety/depression-related behaviours and stress responses (6). It has also been shown that DAG acts in the brain and affects a variety of biological functions, including food intake, gastric emptying and body temperature regulation, as well as glucose and lipid metabolism (7–9). Notably, DAG fails to act on GHSR at physiological ranges (10), and several studies suggest the existence of a specific DAG receptor because some of the effects of DAG occur in a GHSR-independent manner (11). Binding studies have also suggested the existence of a specific receptor for DAG in different cell types, including cardiomyocytes (12), endothelial progenitor cells (13) and foetal rat spinal cord neurones (14), amongst others. Until now, no such receptor has been reported and, consequently, whether DAG is a hormone itself remains a matter of debate. The present study aimed to shed some light on the potential specific actions of DAG in the central nervous system. For this purpose, a DAG fluorescent tracer was used to identify potential brain areas binding this peptide. After confirming that fluorescent DAG specifically labelled a neuronal population located at the arcuate nucleus (ARC), a systematic analysis of the neuroanatomical distribution of DAG labelled cells and their phenotype was performed. To further assess the functional consequences of DAG

action at the ARC, the effect of central administration of DAG on both food intake and expression of the marker of cellular activation c-Fos was tested. All of these parameters were also studied in mice lacking GHSR.

Materials and methods

Animals

Mice were generated in the animal facility of the IMBICE and housed under a 12 : 12 h light/dark cycle (lights on 07.00 h). Animals were kept with regular chow and water available *ad lib*. In the present study, adult (10–12 weeks old) C57BL6/J wild-type (WT) and GHSR-null mice were used. GHSR-null mice were derived from crosses between heterozygous animals back-crossed for more than 10 generations onto a C57BL6/J genetic background (15). The present study was carried out in strict accordance with the recommendations in the Guide for the Care and Use of Laboratory Animals of the National Research Council, and all efforts were made to minimise suffering. All experimentation received approval from the Institutional Animal Care and Use Committee of the IMBICE (approval ID 10-0112).

Reagents

Ghrelin and DAG were purchased from Global Peptide (catalogue no. PI-G-03 and PI-G-04, respectively). Fluorescein-DAG (hereafter named F-DAG) is an 18-amino acid analogue of DAG conjugated to fluorescein isothiocyanate through the addition of a lysine at its C-terminus [Lys(fluorescein)^{19}-DAG (1–19) amide]. F-DAG was provided by Dr L. Luyt from The University of Western Ontario, Canada. The synthesis of F-DAG was carried out in two steps. First, the 19 N-terminal amino acid sequence of ghrelin was synthesised using standard Fmoc solid phase peptide synthesis on Rink amide 4-methylbenzhydrylamine hydrochloride salt resin. Then, the trimethyltrityl orthogonal protecting group present on the lysine at position 19 was deprotected using 2% trifluoroacetic acid and 5% triisopropylsilane in dichloromethane, followed by coupling to fluorescein isothiocyanate isomer I (fluorescein) in the presence of N,N-diisopropylethylamine. Purification was performed by high-performance liquid chromatography to obtain a yellow powder with an overall yield of 23% and a purity of 99%. The final product was characterised by electrospray ionisation time-of-flight mass spectrometry (Xevo QTof MS/Acquity UHPLC; Waters, Milford, MA, USA) with *m/z* determined to be 1309.1565 for $[M + 2H]^{2+}$ (calculated 1309.1087).

Experimental procedures and experiments

To perform F-DAG labelling, mice were stereotaxically implanted with an indwelling sterile guide cannula (length 4 mm, 22-gauge) into the lateral ventricle (i.c.v.). The placement coordinates for the lateral ventricle were: anteroposterior −0.3 mm, lateral +1.0 mm and ventral −2.3 mm. At this anteroposterior level, the lateral ventricles are connected to the third ventricle and i.c.v. injected molecules quickly reach the third ventricle. After surgery, animals were individually housed and allowed to recover for at least 7 days. On the morning of the experimental day, animals were i.c.v. injected with 2 μl of vehicle alone (n = 4) or containing F-DAG (0.3 nmol/mouse, n = 5). The vehicle used in this experiment, as in all experiments described below, was phosphate-buffered saline (PBS) (pH 7.4). To determine the specificity of the labelling method, an additional set of mice were anaesthetised (100 mg/kg ketamine and 10 mg/kg xylazine, i.p.) and i.c.v. injected with 2 μl of vehicle containing 0.12 nmol/mouse of F-DAG alone (n = 3) or plus DAG (1.20 nmol/mouse, n = 3). All i.c.v. injections were made over 2 min through a 30-gauge needle that extend 0.5 mm below the guide cannula, which was connected by polyethylene tubing to a Hamilton syringe. The needle was left in place for 2 min, following the injection, to prevent back flow of the injected solution. Thirty minutes after treatment, mice were perfused with formalin as described previously (16). To study the phenotype of F-DAG-labelled cells, one group of mice was anaesthetised as indicated above and i.c.v. injected with colchicine (16 μg in 4 μl per mouse, n = 4) using the above described coordinates. After for 2 days of recovery, mice were i.c.v. injected with F-DAG, as described above, anaesthetised (500 mg/kg chloral hydrate, i.p.) and perfused 30 min later.

To study the role of DAG on food intake, an independent set of mice were permanently implanted with an indwelling i.c.v. cannula, as described above. i.c.v. cannulated mice were used to test the effect of DAG on food intake during the lights-off cycle and under a fast-refeeding paradigm. After 4–5 days of surgery, the effect of DAG on lights-off cycle food intake was tested in a cross-over design manner. In particular, mice were i.c.v. injected at 18.45 h with 2 μl of vehicle alone or containing 0.3 nmol/mouse of DAG in a randomised alternating scheme on consecutive days (n = 17). The food intake was measured at 22.00 h and 07.00 h of the next day. A similar dose of DAG has been shown to affect food intake in previous studies (7). After 2 days of recovery, animals were exposed to the fast-refeeding paradigm. Initially, food was removed from the home cages at 18.00 h. At 10.00 h the next day, animals were i.c.v. injected with 2 μl of vehicle alone or containing 0.3 nmol/mouse of DAG (n = 8 and 9, respectively) and immediately exposed to a weighed amount of chow. The food intake was measured at 2 and 12 h after re-feeding.

To study the potential interaction between DAG and ghrelin on food intake and ARC c-Fos induction, another set of mice were permanently implanted with an indwelling i.c.v. cannula, as described above. At 10.00 h, animals were i.c.v. injected with 2 μl of vehicle alone or containing 0.3 nmol/mouse of DAG. At 10.15 h, mice were s.c. or i.c.v. injected with a dose of approximately 1.5 (specifically 0.06 nmol/g body weight) or 0.3 nmol/mouse of ghrelin, respectively. The orexigenic effect of these doses of ghrelin has been fully characterised in our previous studies (17). DAG pretreatment was performed 15 min before ghrelin treatment based on the half-life of the peptide, which is approximately 30 min (18). Mice were grouped as: vehicle i.c.v. + vehicle (n = 8), DAG i.c.v. + vehicle (n = 7), vehicle i.c.v. + ghrelin s.c. (n = 20), DAG i.c.v. + ghrelin s.c. (n = 6), vehicle i.c.v. + ghrelin i.c.v. (n = 11) and DAG i.c.v. + ghrelin i.c.v. (n = 6). Two hours after treatment, mice were anaesthetised (500 mg/kg chloral hydrate, i.p.) and perfused as described previously (16). Between injections and sacrifices, mice were exposed to a pre-weighed amount of rodent's food to determine food intake.

To test whether the F-DAG peptide affects food intake and/or c-Fos in the same fashion as seen for the DAG peptide, we performed exactly the same experiment as described above but using F-DAG rather than DAG. Here, a total of 12 WT mice were used and grouped as: vehicle i.c.v. + vehicle s.c. (n = 3), F-DAG i.c.v. + vehicle s.c. (n = 3), vehicle i.c.v. + ghrelin s.c. (n = 3) and F-DAG i.c.v. + ghrelin s.c. (n = 3).

An additional set of experiments were performed with GHSR-null mice. To study F-DAG labelling, GHSR-null mice were anaesthetised (100 mg/kg ketamine and 10 mg/kg xylazine, i.p.) and i.c.v. injected with 2 μl of vehicle alone or containing 0.3 nmol/mouse of F-DAG (n = 3 and 5, respectively) and perfused with fixative 30 min after treatment, as described above. To study food intake and c-Fos induction, an independent set of GHSR-null were i.c.v. injected with 2 μl of vehicle alone or containing 0.3 nmol/mouse of DAG (n = 5 and 6, respectively). Two hours after treatment, mice were also anaesthetised (500 mg/kg chloral hydrate, i.p.) and perfused with fixative.

At the end of all experiments, brains were removed, post-fixed, immersed in 20% sucrose and cut coronally at 42 μm into three equal series on a sliding cryostat. Correct placement of the cannula was confirmed by histological observation.

© 2015 British Society for Neuroendocrinology

F-DAG labelling and its neuroanatomical analysis

Brain sections of F-DAG-injected mice were used for visualisation in a fluorescence microscope and fluorescence immunostaining. For fluorescence immunostaining, brain sections were treated with blocking solution (3% normal donkey serum and 0.25% Triton X in PBS) and incubated with an Alexa-488 anti-fluorescein antibody (catalogue no. A-11096, dilution 1 : 100; Molecular Probes, Carlsbad, CA, USA). Sections were sequentially mounted on glass slides and cover-slipped with mounting media. For double fluorescence immunostaining, brain sections were treated with blocking solution and incubated for 2 days at 4 °C with the anti-fluorescein antibody, as described above, plus one of the following primary antibodies: anti-tyrosine hydroxylase (anti-TH; H-196, catalogue no. sc-14007, dilution 1 : 20 000; Santa Cruz Biotechnology, Santa Cruz, CA, USA), anti-NPY (catalogue no. ab30914, dilution 1 : 7000; Abcam, Cambridge, MA, USA), anti-adrenocorticotrophic hormone (ACTH) [generated and validated by our laboratory (19), dilution 1 : 3000] or anti-vimentin (catalogue no. AB5733, dilution 1 : 2000; Millipore, Billerica, MA, USA). Then, sections were washed and treated with Alexa-594 secondary antibody (catalogue no. A21207 or A11042, dilution 1 : 1000; Molecular Probes) for 2 h. Then, sections were washed, sequentially mounted on glass slides, and coverslipped with mounting media. Fluorescence images were acquired, in comparable areas under the same optical and light conditions, with an Eclipse 50i epifluorescence microscope and a DS-Ri1 Nikon digital camera (Nikon, Tokyo, Japan). For neuroanatomical analysis, anatomical limits of the different brain regions were identified by comparison to a mouse brain atlas (20) using the same mounted series imaged for fluorescence, for which the coverslip was carefully removed, and the mounted slices were washed, stained with thionin (catalogue no. T7029; Sigma-Aldrich, St Louis, MO, USA), dehydrated in an ascending alcohol series, cleared in xylene and re-coverslipped. To estimate the total number of F-DAG-labelled cells in the ARC, cells containing a distinct fluorescence signal were quantified in one out of three complete series of coronal sections through the whole nuclei. Then, these numbers were summed and multiplied by three. The data were corrected for double counting, according to the method of Abercrombie (21), where the ratio of the actual number of neurones to the observed number is represented by T/T + h where T is section thickness, and h is the mean diameter of the neurone. For this, F-DAG-labelled cell diameter was quantified using FIJI (NIH, Bethesda, MD, USA). To estimate fluorescence signal intensity in the ARC, 16-bit colour microphotographs were acquired with a filter cube with a long-pass emission filter (Nikon B/2A) and flat-field corrected using a reference image from a homogeneously fluorescent slide. Then, to compensate for tissue autofluorescence a new image was generated by subtracting from the green channel of the original image a fraction of the red channel to obtain an average signal of zero in an unstained region of the parenchyma. Finally, the mean fluorescence intensity was quantified in the whole ARC. All the image processing and quantification was performed in FIJI. In double-immunostained sections, the total number of green fluorescence and/or red fluorescence labelled cells was quantified in ARC slices ranging from bregma −1.64 to −1.88, where the F-DAG-labelled cells were concentrated (see Results). In particular, approximately 800 cells were counted in four mice. Using these cell counts, the percentage of DAG-labelled cells containing red fluorescence and the percentage of each type of red fluorescence labelled cells positive for DAG-labelling were calculated as: (number of cells with co-localisation/total number of DAG-labelled cells) × 100 and (number of cells with co-localisation/total number of red fluorescence labelled cells) × 100, respectively.

c-Fos immunostaining and its neuroanatomical analysis

Brains sections were pretreated with H_2O_2, treated with blocking solution and incubated with a rabbit anti-c-Fos antibody (H-125, catalogue no. sc-7202, dilution 1 : 4000; Santa Cruz Biotechnology) for 2 days at 4 °C. Then, sections were incubated with biotinylated donkey anti-rabbit antibody (catalogue no. BA-1000, dilution 1 : 1500; Vector Laboratories, Inc., Burlingame, CA, USA), and with Vectastain Elite ABC kit (catalogue no. PK-6200; Vector Laboratories, Inc.), in accordance with the manufacturer's instructions. The visible signal was developed with diaminobenzidine/nickel solution (catalogue no. 32750; Sigma-Aldrich), which generated a black precipitate. Finally, sections were mounted on glass slides and coverslipped with mounting media. To assess c-Fos induction following DAG or F-DAG treatment, independent blind quantitative analysis was performed manually by two observers in comparable areas under the same optical and light conditions. The number c-Fos-immunoreactive (-IR) cells in the whole ARC was determined by quantifying the cells containing a distinct nuclear black precipitate between bregma −1.22 and −2.46 mm, using the neuroanatomical references described above, in one-in-three series. The c-Fos-IR nuclei corresponding to the ependymal epithelium were excluded from the analysis. Quantitative analysis was performed in each side of ventricle and expressed as total c-Fos-IR cells per side and per section. For the topological analysis of c-Fos-IR cells distribution within the ARC, a digital imaging approach was implemented. Bright-field images were acquired for brain slices ranging from bregma −1.64 to −1.88, where c-Fos-IR cells where concentrated, using the same microscope and camera as stated above. On each image, two squares (400 × 400 μm) were delimited, one over each ARC. Specifically, the ventral limit of brain and the ventricular wall were used as alignment references for the bottom and medial borders, respectively, of each ARC. Each square was subdivided into four equal-sized quadrants; thus, the upper quadrant close to the ventricle corresponds to the dorsal ARC subregion (dARC), whereas the bottom quadrants located close or distant of the ventricle correspond to the ventromedial ARC (vmARC) or ventrolateral ARC (vlARC) subregions, respectively. For the quantitative analysis, the position of every c-Fos-IR cell within each quadrant was manually recorded, excluding those belonging to the ependymal wall. Then, the number of c-Fos-IR cells per sample per quadrant was calculated by averaging all the corresponding quadrants (left and right) belonging to images of the same sample. Finally, the average c-Fos-IR cell count for the three quadrants was calculated for each experimental group. To further obtain an overall c-Fos-IR spatial distribution, each square was subdivided in a 32 × 32 grid of bins (12.5 μm by side) and the average c-Fos-IR cell number per bin was computed for each experimental group. The final result was rendered as colour-coded density maps. All these procedures were performed using FIJI.

c-Fos/ACTH or c-Fos/TH immunostaining and its neuroanatomical analysis

Double c-Fos and TH or c-Fos and ACTH immunostainings were performed on independent brain series. In this case, sections were incubated with either the rabbit anti-TH antibody (dilution 1 : 20 000) or the rabbit anti-ACTH antibody (dilution 1 : 6000) for 48-h after c-Fos immunostaining was completed. Next, sections were sequentially incubated with a secondary antibody and the Vectastain Elite ABC kit, as described above. Visible signal was developed with diaminobenzidine solution without nickel, generating a brown precipitate. Finally, sections were mounted on glass slides and coverslipped with mounting media. The number of double-labelled c-Fos/TH or c-Fos/ACTH neurones in the ARC was quantified in a complete series of each animal. TH and ACTH immunostaining were confined to the perikarya, thus allowing the easy visualisation of the c-Fos-positive nuclei. To estimate the amount of each type of neurones positive for c-Fos, ACTH-IR and TH-IR cells with positive or negative cell nucleus for c-Fos immunostaining were counted in the ARC. The proportion was expressed as a percentage, which represents ACTH-IR or TH-IR neurones positive for c-Fos compared to the total number of IR neurones observed.

© 2015 British Society for Neuroendocrinology

Statistical analysis

Data are expressed as the mean ± SEM. Equality of variance was analysed using Bartlett's test. A t-test was performed to compare data from vehicle- versus DAG-treatment in WT or GHSR-null mice, as well as the effect of DAG on fluorescent F-DAG labelling intensity. A two-way repeated measures ANOVA (time × treatment) followed by the Bonferroni test was used to compare the impact of i.c.v. DAG treatment on dark cycle food intake and refeeding phase after overnight fasting. Two-way ANOVA (pretreatment × treatment) followed by the Bonferroni test was used to compare the impact of vehicle or DAG i.c.v. pretreatments an further vehicle, ghrelin s.c. or ghrelin i.c.v. treatments on food intake and c-Fos induction (pretreatment × treatment). $P < 0.05$ was considered statistically significant. Analyses were performed using PRISM, version 5.0 (GraphPad Software Inc., San Diego, CA, USA).

Results

F-DAG labels and acts on ARC cells

To reveal the brain areas directly responsive to DAG, mice were i.c.v. injected with either vehicle or F-DAG, and the coronal brain sections were examined under a fluorescence microscope. Under this condition, a strong cell body-shaped green fluorescence signal was observed exclusively in the F-DAG-injected mice and no signal was observed in vehicle-treated mice. The brain area with the highest labelling was the ARC. To enhance and stabilise the fluorescence signal, fluorescence immunostaining against fluorescein was performed. Immunostaining showed specificity because no signal was observed in brain samples from vehicle-treated mice (Fig. 1). In addition, the fluorescein-IR signal was significantly reduced by an excess of unlabelled DAG; in particular, the mean fluorescence intensity in the ARC of mice treated with F-DAG and DAG was 35 ± 7% of that detected in mice treated with F-DAG alone (100 ± 11%, $P < 0.05$).

From a neuroanatomical standpoint, F-DAG-labelled cells were mainly found at the ARC and distributed between rostrocaudal levels −1.22 and −2.46 mm from bregma (Fig. 2A–C). In total, approximately 500 F-DAG-labelled cells were estimated in the ARC. F-DAG-labelled cells were concentrated in the vmARC in close apposition to the median eminence (ME). The F-DAG-labelled cells were predominantly medium-sized (approximately 12.5 μm) with an intense fluorescence signal mainly located in the cell bodies. Intense F-DAG-labelled cells were also located in the ependymal layer lining the walls of the third ventricle, mostly in the floor of the infundibular recess. However, to a much lesser extent and lower intensity, F-DAG-labelled cells were also found scattered in the area postrema and other hypothalamic and extra-hypothalamic areas, particularly near the ventricles (e.g. the dorsomedial hypothalamic nucleus). Notably, no positive cells were found in the hippocampus, cerebellum or cerebral cortex.

To test whether F-DAG acts on ARC neurones, the effect of i.c.v. F-DAG on c-Fos induction was analysed. A significant increase in the number of c-Fos-IR cells was detected in the ARC of F-DAG-injected mice compared to values detected in vehicle-injected mice (42 ± 5 and 14 ± 2 c-Fos-IR cells/section, respectively, $P < 0.05$). Because the fluorescein moiety could impact on c-Fos induction and also the tracer is a shorter form of intact DAG, the effect of i.c.v. native DAG on c-Fos induction was also analysed. A significant increase in the number of c-Fos-IR cells was also detected in the ARC of DAG-injected mice compared to values detected in vehicle-injected mice. In particular, 9 ± 2 and 28 ± 4 c-Fos-IR cells/section were estimated in the ARC of vehicle and DAG-injected mice, respectively ($P < 0.01$) (Fig. 2D). Notably, c-Fos-IR cells were mainly located in the vmARC, with a similar pattern of distribution as that seen for the F-DAG-labelled cells. In addition to the ARC, a significant increase in the number of c-Fos-IR cells was also detected in the paraventricular nucleus (PVN) (not shown).

F-DAG labels ARC NPY neurones

To reveal the phenotype of ARC F-DAG-labelled cells, brain slices from mice pretreated with colchicine and then i.c.v. injected with F-DAG were used to perform double immunostaining. The pattern of F-DAG labelling was unaffected by colchicine pretreatment. Double-labelled neurones were detected when co-immunostaining was performed using anti-fluorescein and anti-NPY antibodies (Fig. 3A). The quantification of the degree of co-localisation of both fluorescence signals indicated that 33 ± 4% of NPY-IR cells also were labelled by F-DAG. Notably, 78 ± 4% of F-DAG labelled cells were not NPY-IR cells. By contrast, no double-labelled neurones were detected when co-immunostaining was performed against fluorescein and either a marker of pro-opiomelanocortin (POMC)

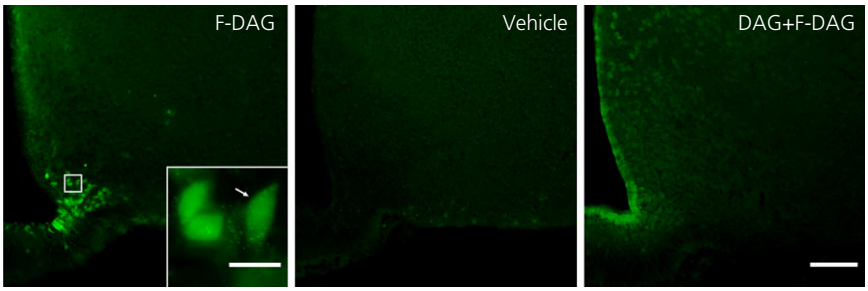

Fig. 1. Fluorescein-des-acyl ghrelin (F-DAG) specifically binds to the arcuate nucleus (ARC) of wild-type (WT) mice. Representative photomicrographs are shown of the fluorescein-immunoreactive (-IR) signal in ARC coronal sections of WT mice that were i.c.v. injected with F-DAG (left), vehicle (middle) or F-DAG plus DAG (right), and perfused 30 min later. The inset shows a high magnification image of the area marked in the low magnification image. Arrow indicates a fluorescein-IR cell. Scale bars = 100 μm (low magnification), 15 μm (high magnification).[

© 2015 British Society for Neuroendocrinology

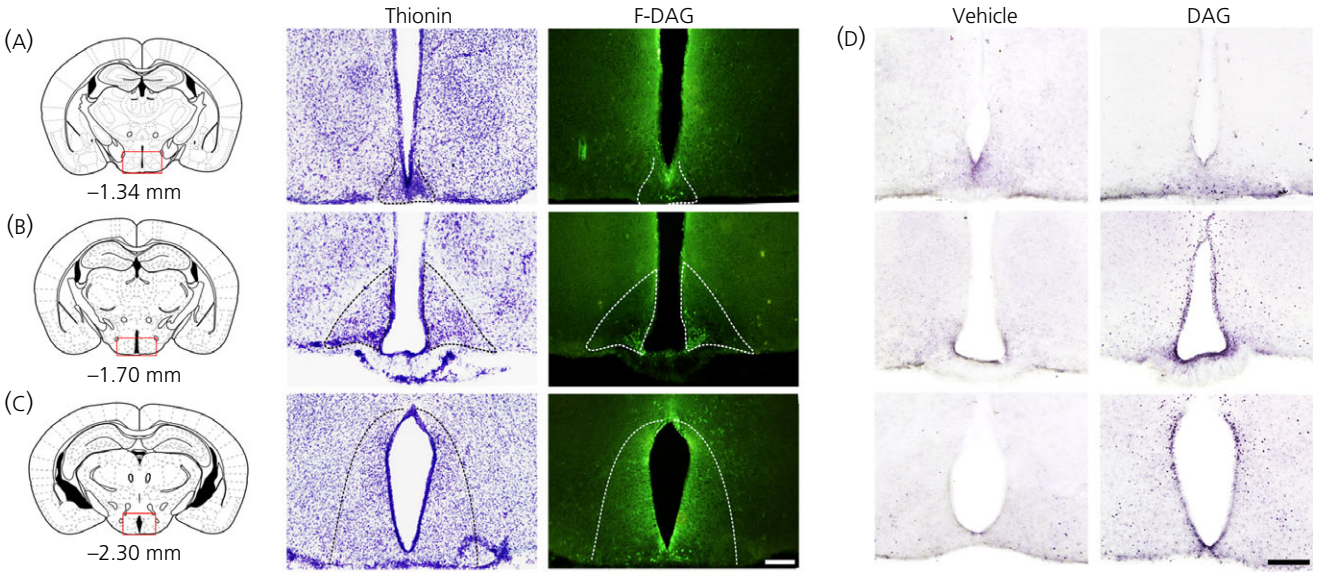

Fig. 2. Detailed distribution pattern of fluorescein-des-acyl ghrelin (F-DAG)-labelled cells and DAG-induced c-Fos-immunoreactive (-IR) cells within the rostro-caudal levels of the arcuate nucleus (ARC) of wild-type mice. A set of representative images is shown from the anterior (A), middle (B) and posterior (C) levels of the ARC containing F-DAG binding neurones. For each level, a diagram of the corresponding coronal section is shown (left), with a rectangle indicating the approximate region from where the images were obtained, along with microphotographs of the thionin-staining of the coronal brain sections (centre) and the subsequent anti-fluorescein immunohistochemistry on the same sections (right). (D) A set of representative images of c-Fos-IR cells in the same anterior, middle and posterior levels of the ARC of vehicle- (left) or DAG-treated (right) mice. Scale bars = 100 μm.

neurones (anti-ACTH) (Fig. 3B) or a marker of dopaminergic neurones (anti-TH, not shown). Interestingly, F-DAG-labelled cells located in the ependymal layer were positive for anti-vimentin immunostaining, suggesting that they are tanycytes (Fig. 3D). Within tanycytes, a F-DAG signal was found in the cell body, as well as in their cellular processes that extend into the ME.

F-DAG labels and acts on ARC cells of GHSR-deficient mice

To test whether DAG labelling depends on the ghrelin receptor, GHSR deficient mice were i.c.v. injected with vehicle or F-DAG, and the brain sections immunostained as described above. As seen in WT mice, fluorescent cells were detected in F-DAG-injected mice, with the ARC demonstrating the highest labelling (Fig. 4A). To test whether DAG activates ARC cells in a GHSR independent fashion, c-Fos induction was analysed in GHSR-null mice i.c.v. treated with vehicle or DAG. As seen in WT mice, DAG-injected GHSR-null mice showed a significant increase in the number of c-Fos-IR cells compared to the numbers found in vehicle-injected GHSR-null mice in the ARC (31 ± 4 and 3 ± 1 cells/section, respectively, $P < 0.01$) (Fig. 4B), as well as in the PVN (not shown). Food intake of GHSR-null mice was not affected by i.c.v. DAG treatment.

i.c.v. DAG impairs the orexigenic actions of peripherally administered ghrelin

Because DAG impacts on the ARC, we tested whether i.c.v. DAG affects food intake. Previous studies have shown that DAG can inhibit food intake; thus, the effect of DAG on food intake was tested in WT under conditions with high food intake, including during the dark phase of the day and after a period of fasting. However, i.c.v. DAG failed to affect spontaneous food intake in *ad lib.* fed mice during the dark phase (Fig. 5A), as well as during the refeeding phase after overnight fasting (Fig. 5B). Because ARC neurones are a main target of orexigenic actions of ghrelin, the potential interaction between DAG and ghrelin on food intake was tested. The effect of i.c.v. DAG pretreatment was tested in mice treated either peripherally or centrally with ghrelin (Fig. 5C). Two-way ANOVA for 2-h food intake revealed a significant interaction between i.c.v. pretreatment and further treatment ($F_{2,52} = 3.220$, $P < 0.05$). In particular, i.c.v. DAG treatment significantly reduced 2-h food intake increase induced by peripheral administration of ghrelin compared to vehicle-treated mice ($P < 0.01$). Interestingly, i.c.v. DAG treatment failed to affect 2-h food intake increase induced by i.c.v. administration of ghrelin. Notably, the i.c.v. pretreatment with F-DAG also significantly reduced the 2-h food intake increase induced by peripheral administration of ghrelin (143 ± 24 versus 470 ± 31 mg, respectively, $P < 0.01$).

DAG and ghrelin differentially increase c-Fos at ARC subregions

To obtain insight into the potential mechanism mediating DAG-induced impairment of the orexigenic effect of peripherally administered ghrelin, the number of ARC c-Fos-IR cells was analysed within the ARC subregions of the above described experimental groups treated with DAG and/or ghrelin (Fig. 6A,B). Two-way ANOVA analysis for the number of c-Fos-IR cells in each subregion

© 2015 British Society for Neuroendocrinology

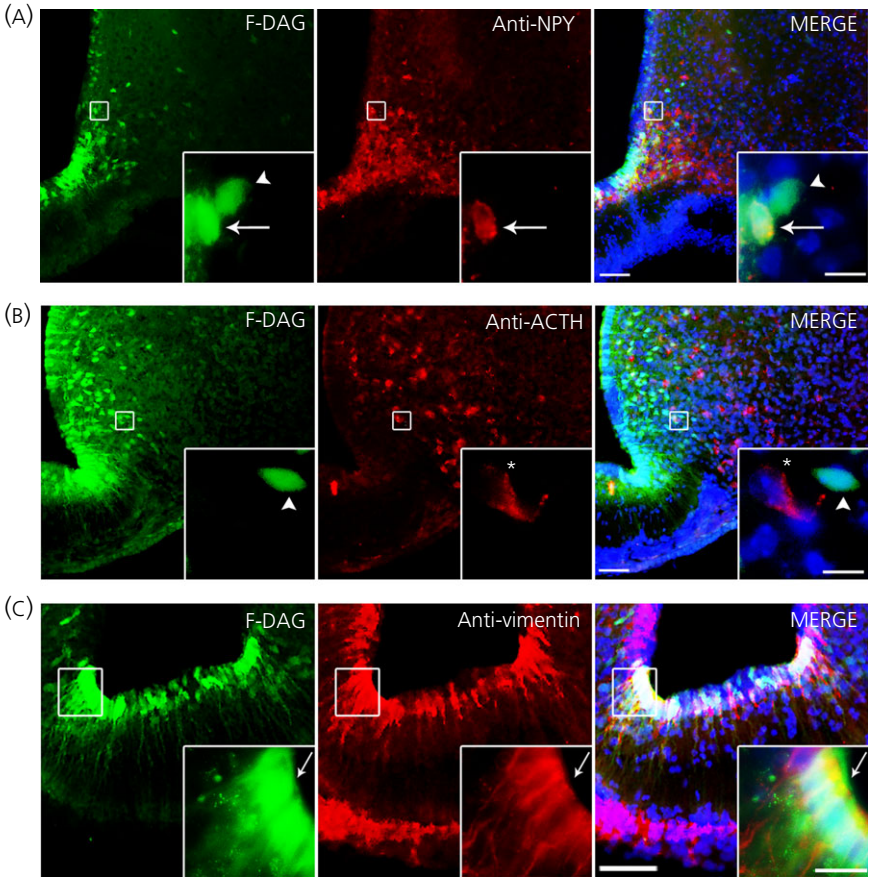

Fig. 3. Fluorescein-des-acyl ghrelin (F-DAG) labels neuropeptide (NPY)-immunoreactive cells. A set of representative images is shown of arcuate nucleus (ARC) (A, B) and ME (C) areas of a mouse i.c.v.-injected with F-DAG and then subjected to double fluorescent immunohistochemistry using green anti-fluorescein and anti-NPY (A), anti-adrenocorticotrophic (ACTH) (B) or anti-vimentin (C) antibodies that were subsequently visualised with a secondary red antibodies; sections were also counterstained using Hoechst (blue) to visualise cell nuclei. For each panel, low and high magnification images are shown for the green (left), red (middle) and green-red-blue merged (right) channels. Arrows indicate dual-labelled cells. Arrowheads indicate singly F-DAG-labelled cells. The asterisk labels a neurone singly labelled by anti-ACTH antibody Scale bars = 100 μm (low magnification), 10 μm (high magnification).

indicated a different topographic distribution for the number c-Fos positive between groups. In the dARC (Fig. 6C), two-way ANOVA revealed a main effect of both pretreatment ($F_{1,21} = 9.42$, $P = 0.006$) and treatment ($F_{2,21} = 8.92$, $P = 0.002$). However, no significant interaction between pretreatment and treatment was found ($F_{2,21} = 0.111$, $P > 0.05$). Similar results were observed in the vlARC (Fig. 6E), where two-way ANOVA revealed a main effect of both pretreatment ($F_{1,21} = 14.43$, $P = 0.001$) and treatment ($F_{2,21} = 36.46$, $P < 0.0001$). In particular, mice i.c.v. injected with ghrelin display a significant increase in the number of c-Fos-IR cells compared to vehicle-injected mice ($P < 0.05$). Here, no significant interaction between pretreatment and treatment was found ($F_{1,21} = 1.31$, $P > 0.05$), although i.c.v. ghrelin induced a significant increase in the number of c-Fos-IR cells for both pretreatments ($P < 0.001$). Interestingly, very robust differences were found in the vmARC (Fig. 6D), where significant differences were induced by i.c.v. pretreatment ($F_{1,21} = 80.88$, $P < 0.0001$) or further treatment ($F_{2,21} = 142.9$, $P < 0.0001$). Here, i.c.v. DAG treatment induced a further increase in the number of c-Fos-IR cells induced by either vehicle ($P < 0.01$), ghrelin s.c. ($P < 0.001$) or ghrelin i.c.v. ($P < 0.001$). Importantly, no significant interaction between i.c.v. pretreatment and further treatment was revealed in the vmARC ($F_{2,21} = 2.32$, $P > 0.05$); thus, the number of c-Fos-IR cells in this ARC subregion of mice pretreated with i.c.v. DAG is increased in a similar fashion compared to their own vehicle-treated group, independent of further treatment.

Because DAG and ghrelin could act on different ARC cells, which may differentially impact on food intake, we tested the effect of ghrelin and DAG on POMC neurones. For this purpose, double immunostaining using anti-ACTH and anti-c-Fos antibodies was performed in brain slices from mice i.c.v. treated with vehicle, ghrelin or DAG (Fig. 6). Compared to vehicle treatment, i.c.v. DAG and i.c.v. ghrelin induced a significant increase in the number of ACTH-IR neurones positive for c-Fos ($P < 0.05$) that was not different between them. In particular, 3.2 ± 1.0%, 6.4 ± 0.6% and 5.9 ± 0.2% of ACTH-IR cells were positive for c-Fos in the ARC of vehicle, ghrelin or DAG treated animals, respectively. Notably, c-Fos positive ACTH-IR cells represented 17.7 ± 2.8% and 2.8 ± 0.3% of all c-Fos-IR cells within the ARC of DAG and ghrelin-treated mice, respectively ($P < 0.05$). Additionally, a double immunostaining using

© 2015 British Society for Neuroendocrinology

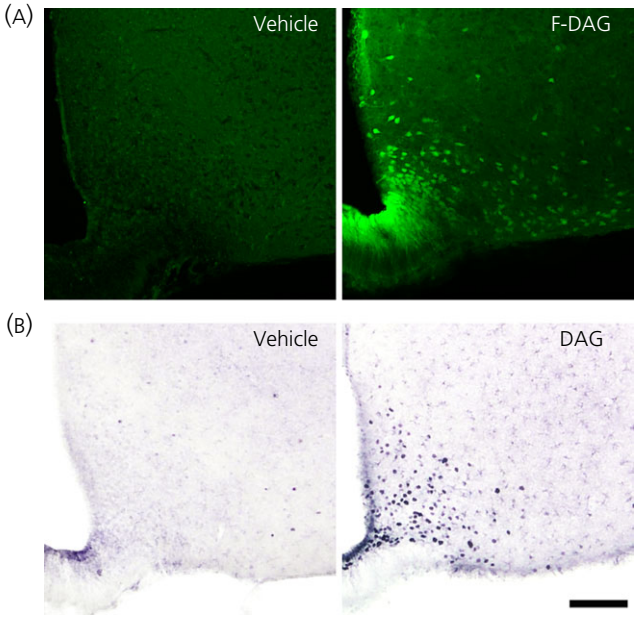

Fig. 4. Fluorescein-des-acyl ghrelin (F-DAG) labels and acts on arcuate nucleus (ARC) cells of growth hormone secretagogue receptor (GHSR)-deficient mice. (A) Representative photomicrographs of fluorescein-immunoreactive (-IR) signal in ARC coronal sections of GHSR-deficient mice that were i.c.v. injected with vehicle (left) or F-DAG (right). (B) Representative photomicrographs of c-Fos-IR signal in ARC of GHSR-deficient mice that were i.c.v. injected with vehicle (left) or DAG (right). Scale bar = 100 μm.

anti-TH and anti-c-Fos antibodies was performed in samples of the same experimental groups; however, no significant changes in the number of TH-IR neurones positive for c-Fos were found between them (not shown).

Discussion

In the present study, we provide the first evidence that DAG directly targets the ARC neurones. Consistent with an action on food intake-regulating neurones, we found that DAG impairs the orexigenic actions of peripherally administered ghrelin. Notably, F-DAG labelled and activated the ARC neurones of GHSR deficient mice. Thus, these data support the notion that a specific DAG receptor exists and suggest that DAG plays an anorexigenic role in a GHSR-independent manner.

The peptide tracer used here is a 19-amino acid analogue of the N-terminal side of DAG conjugated to a molecule of fluorescein at its C-terminus. F-DAG labelling was reduced by an excess of unlabelled DAG, suggesting that the tracer was specific and, consequently, an accurate tool for imaging DAG binding sites. Notably, the observation that F-DAG both increased c-Fos levels and blocked the orexigenic effect of peripherally administered ghrelin, similar to that seen for DAG, also suggests that the fluorescent tracer is fully bioactive. As seen for the binding region of ghrelin to GHSR (10), the binding region of DAG to its putative receptor would be located within the N-terminal amino acids because the chemical structure of the N-terminus of the tracer is the same compared to that of

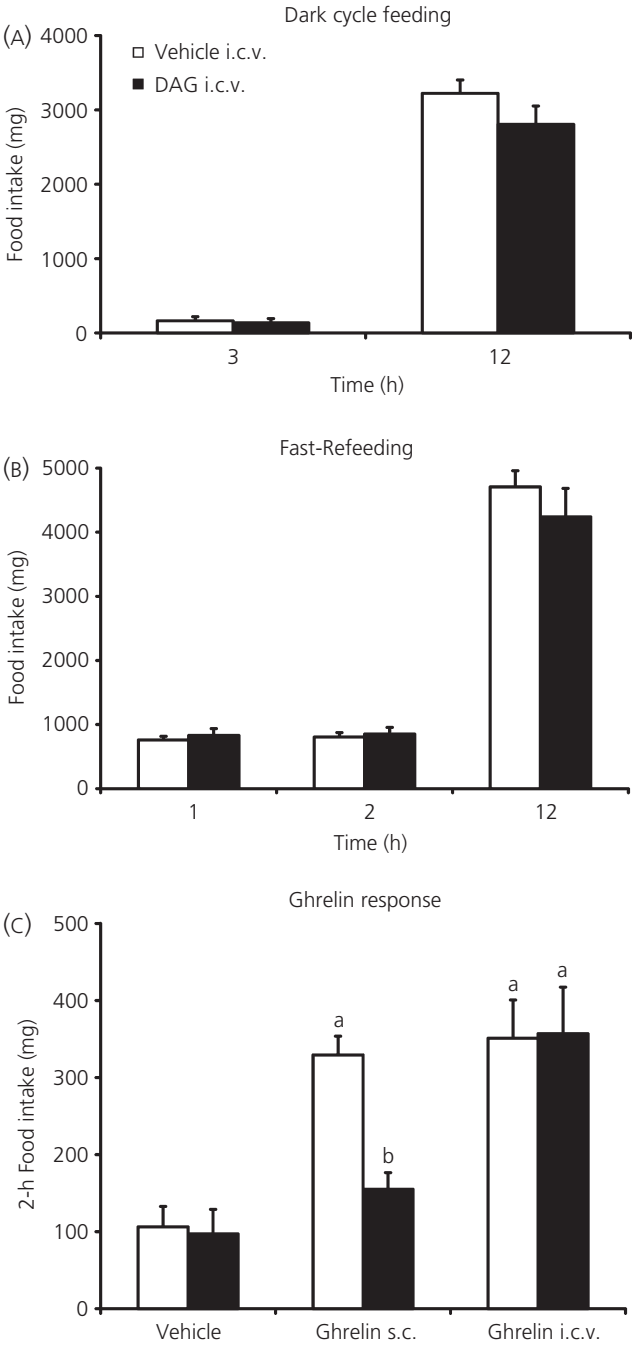

Fig. 5. Des-acyl ghrelin (DAG) impairs the orexigenic actions of peripherally administered ghrelin. (A) Showing 2- and 12-h dark cycle food intake in mice that were i.c.v. treated with vehicle or DAG. (B) Showing 1-, 2- and 12-h food intake in mice that were initially fasted and then i.c.v. treated with vehicle or DAG just before re-feeding. (C) Showing 2-h food intake in mice that were first i.c.v. pretreated with vehicle or DAG and subsequently treated with either vehicle, ghrelin s.c. or ghrelin i.c.v. Values are the mean ± SEM and were compared by a two-way ANOVA. $^{a}P < 0.05$ versus vehicle-pretreated and same treatment. $^{b}P < 0.05$ versus same pretreatment followed by vehicle.

intact DAG. A receptor specificity located at the N-terminus of these peptides appears to be expected because this side is the only region where these molecules differ by the presence of the octanoyl

© 2015 British Society for Neuroendocrinology

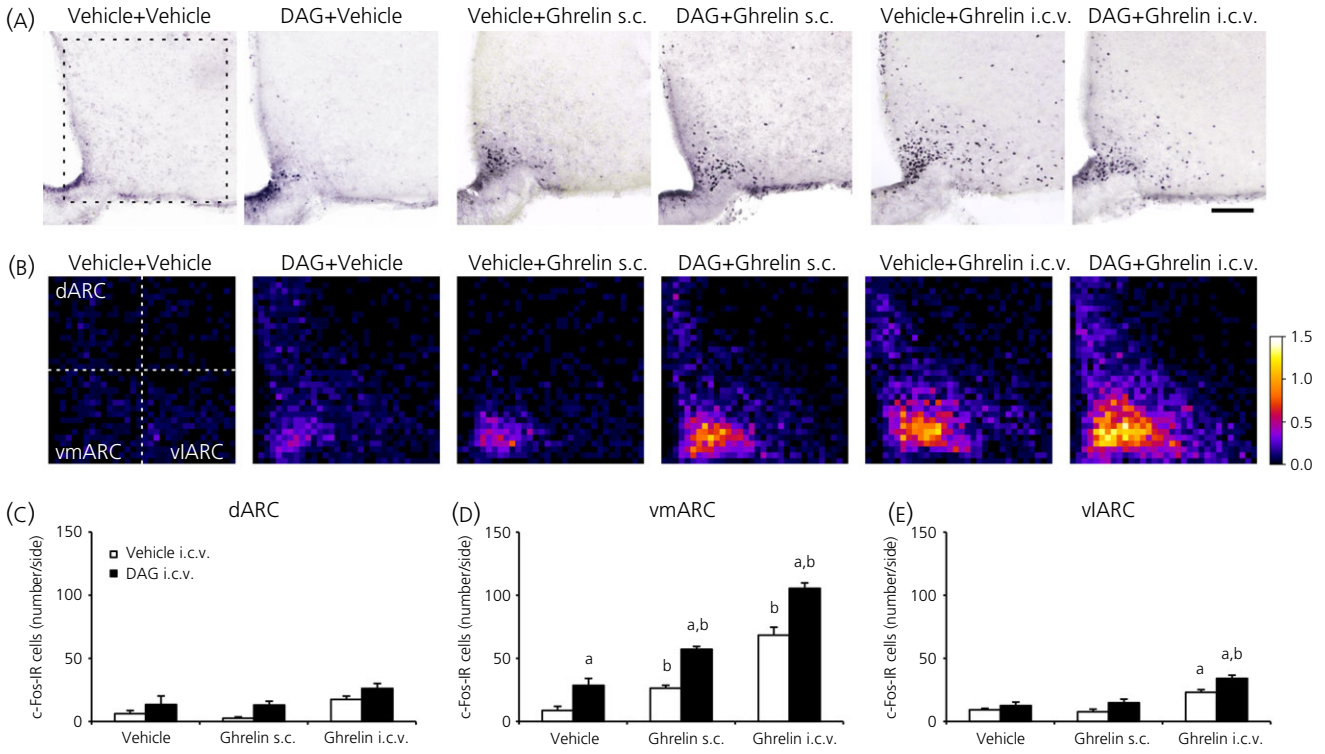

Fig. 6. Des-acyl ghrelin (DAG) and ghrelin induce c-Fos differentially in specific arcuate nucleus (ARC) subregions. (A) Showing representative low magnification images of c-Fos immunostaining in the ARC of mice that were first i.c.v. pretreated with vehicle or DAG and subsequently treated with either vehicle, ghrelin s.c. or ghrelin i.c.v.. (B) Showing the average c-Fos-immunoreactive (-IR) cell density within a square region (400 × 400 μm) comprising the ARC for each experimental group. The placement of this region is indicated in (A) by a dashed square. Density is expressed as c-Fos-IR cells/bin of side 12.5 μm. (C–E) Quantitative analysis of the number of c-Fos-IR cells in the dorsal ARC subregion (dARC), ventromedial ARC (vmARC) and ventrolateral ARC (vlARC) subregions of mice of each experimental group. Values are expressed as the mean ± SEM and were compared by a two-way ANOVA. [a]$P < 0.05$ versus vehicle-pretreated and same treatment. [b]$P < 0.05$ versus same pretreatment followed by vehicle. Scale bar = 100 μm.

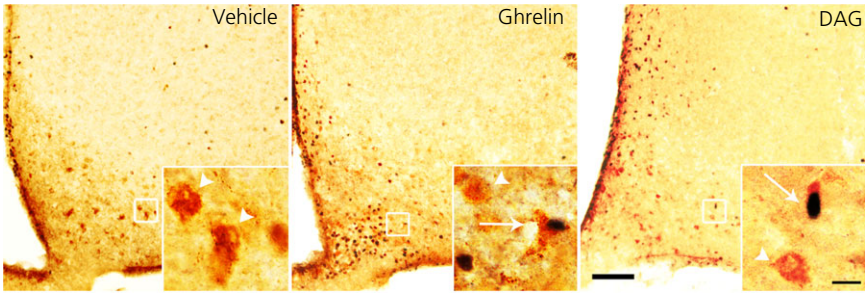

Fig. 7. Des-acyl ghrelin (DAG) and ghrelin induce c-Fos expression in pro-opiomelanocortin arcuate nucleus (ARC) neurones. Representative photomicrographs are shown of ARC sections subjected to double immunohistochemistry using anti-adrenocorticotrophic hormone (brown signal) and anti-c-Fos (black signal) antiserum. Brain samples correspond to wild-type (WT) mice that were i.c.v. injected with vehicle (left), ghrelin (middle) or DAG (right), and perfused 2-h later. The insets show a high magnification image of the area marked in the low magnification images. Arrowheads point to single-labelled cells, and arrows point to dual-labelled cells. Scale bars = 100 μm (low magnification), 10 μm (high magnification).

group. Interestingly, F-DAG-labelled cells were found in the brain of GHSR deficient mice, indicating that the presence of GHSR is not required for DAG labelling. Actions of DAG independent of GHSR have been already suggested. For example, central infusion of DAG regulates body temperature in the presence of a GHSR antagonist (8), and DAG is able to regulate clusters of genes involved in glucose and lipid metabolism in GHSR-deficient mice (22). As described in the Introduction, binding studies in some cell types have also suggested the existence of a specific DAG receptor (12–14). To our knowledge, however, the results of the present study are the first to show that DAG specifically binds to hypothalamic neurones by a putative receptor different from GHSR.

The results of the present study indicate that the key hypothalamic targets of DAG include a subset of ARC neurones and

© 2015 British Society for Neuroendocrinology

tanycytes. ARC DAG-labelled cells included NPY neurones and another unidentified cell type, both of which were located at close apposition to the ME and therefore are well situated to sense circulating DAG. ARC F-DAG-labelled NPY neurones may mediate the effects of DAG on food intake regulation because NPY neurones play a critical role in this regard (23,24). The majority of ARC NPY neurones express GHSR (25), and ARC neurones are the only cell type, within the whole brain, expressing both GHSR and leptin receptors (15). Thus, a particular set of ARC neurones appears to be highly specialised to integrate peripheral signals affecting energy balance. Notably, F-DAG also labelled cells that were non-NPY, non-POMC and non-dopamine neurones, indicating that DAG may directly impact on another unknown type of ARC neurones. As discussed below, POMC neurones may be an indirect target of DAG. By contrast, dopamine neurones do not appear to be an indirect target of DAG either, at least based on the observation that i.c.v. DAG treatment failed to increase c-Fos in ARC TH-IR neurones. In the present study, we also report that i.c.v. injected F-DAG labelled tanycytes were lining the floor of the third ventricle. Hypothalamic tanycytes are specialised bipolar ependymal cells that bridge the cerebrospinal fluid and ME capillaries. Thus, the observation in the present study suggests that tanycytes would be able to transport DAG through the blood–cerebrospinal fluid barrier. In this regard, we have shown that fluorescent ghrelin can be detected in the tanycytes of animals injected with this tracer (17,26). In addition, hypothalamic tanycytes can take up circulating leptin from the ME and transport it to the cerebrospinal fluid (27). Because DAG rapidly accesses the brain (28), it is possible that tanycytes may play a relevant role in the blood to brain transport of DAG. Importantly, faint F-DAG-labelled cells were also found in other brain areas of F-DAG-treated mice; however, this labelling was less intense compared to ARC neurones. It is important to emphasise that the number, location and fluorescence signal of F-DAG-labelled cells in the present study depended on the accessibility of the i.c.v. injected tracer to the brain parenchyma; thus, our results do not allow us to rule out the possibility that other DAG direct targets exist in the mouse brain.

Actions of DAG at the ARC level could mediate the previously reported anorexigenic effects of DAG administration because this hypothalamic nucleus is a well-established regulator of appetite (29). In rodents, it has been reported that DAG decreases food intake during the dark phase cycle or after food deprivation (7,30). An anorexigenic role of DAG is consistent with the phenotype of transgenic mice overexpressing ghrelin gene in cell types that lack GOAT expression. These mutant mice display elevated plasma DAG concentrations, rather than elevation of ghrelin levels, as well as reduced food intake, body weight, fat mass and nose-to-anus length (31). In the present study, we also tested the effect of i.c.v. DAG on dark phase feeding, as well as food intake, after a starvation period, both representing conditions in which food intake is elevated, and therefore facilitating the detection of an inhibitory effect of this peptide. DAG was centrally injected to rule out any potential contribution of the peripheral actions of the peptide to our observations. Under our experimental conditions, we could not detect any significant effect of i.c.v. DAG on food intake. Our results are not completely unexpected because other studies have also failed to detect inhibitory effects of DAG on the food intake of animals either *ad lib.* fed or re-fed after fasting (32–34). The lack of effect of i.c.v. DAG on food intake in the present study does not appear to depend on the dose of peptide (0.3 nmol/mouse) because another study using a wide range of DAG dose (0.04–5.00 nmol/mouse/day) has also failed to detect effects on food intake (9). The reason for the inconsistency of the available data concerning the effects of DAG on spontaneous food intake is unclear. Importantly, we were able to unmask an anorexigenic effect of DAG by showing that this dose of DAG reduces food intake induced by peripherally administered ghrelin. Similar results were previously reported in other studies using peripheral administration of DAG (33); thus, our observations suggest that DAG impairs ghrelin orexigenic effect by acting centrally (33,35). In addition, our data suggest that DAG impairs ghrelin-evoked GHSR activation, rather than constitutive GHSR activity, because no effects of DAG were detected when ghrelin was not exogenously administered.

The physiological implications of the effect of DAG on the actions of ghrelin at the hypothalamic level are currently uncertain. Some studies have suggested that ghrelin and DAG can be centrally produced (36); however, the source of these peptides in the hypothalamus appears to be mainly from the circulation (37). Plasma levels of both peptides increase almost at the same time (i.e. prior to periods of high food intake at the beginning and end of the dark cycle in rodents) (38). Despite DAG and ghrelin being secreted together from the stomach, DAG is also quickly produced in the circulation by de-acylation of ghrelin (3). In addition, the DAG half-life is longer than the ghrelin half-life (18). Thus, it can be hypothesised that DAG may work as a modulator of ghrelin signalling, limiting its biological actions. Interestingly, we found that DAG binds to and acts on ARC cells of GHSR-deficient mice. Unfortunately, we have been unable to unmask an effect of DAG on the food intake in these mutant mice because DAG failed to affect food intake in WT mice (thus, no effect on GHSR-deficient mice is expected) and the effect of DAG impairing the orexigenic effect of ghrelin cannot be tested in GHSR-deficient mice. Importantly, DAG was shown to regulate the genes involved in lipid and carbohydrate metabolism in the liver, muscle and white adipose of GHSR-deficient mice (22). In addition, it has been suggested that ghrelin regulates some of these metabolic pathways via its hypothalamic action (39). Indeed, selective expression of GHSR in ARC AgRP neurones is sufficient to mediate the effects of ghrelin on glycaemia (40). Thus, GHSR-null mice may be useful for clarifying the physiological role of DAG when acting at in the hypothalamus.

The present study provides important insights into the mechanisms by which i.c.v. DAG could impair the orexigenic action of ghrelin. F-DAG-labelled cells are mainly found at the ARC and i.c.v. DAG increased c-Fos only in the ARC and the PVN. Notably, i.c.v. DAG impaired the increase in food intake induced by peripherally administered ghrelin, whereas it failed to affect the orexigenic effect of centrally administered ghrelin. We have previously shown that acute elevations of plasma ghrelin mainly impact at the ARC, where NPY neurones are critical for its orexigenic effects, and that ARC-ablated mice fail to increase food intake in response to

 © 2015 British Society for Neuroendocrinology

peripherally administered ghrelin (17,40–42). By contrast, centrally administered ghrelin accesses and activates a variety of brain nuclei, which can mediate the orexigenic effects of the hormone even in the absence of an intact ARC (17). Thus, the food intake results in the present study, together with the neuroanatomical data, suggest that DAG can impair the actions of ghrelin on ARC neurones but not in other brain targets of ghrelin. In addition, the topological analysis of the distribution of c-Fos positive cells within the ARC allows us to clarify some aspect of the interaction between these two peptides. We confirmed in the present study that both DAG and ghrelin increase c-Fos in the ARC, as reported previously (7,17). To affect food intake, DAG and ghrelin could impact on the same or on different ARC cells. F-DAG-labelled neurones and c-Fos induction in response to DAG occurs in the vmARC, where NPY neurones are predominantly located (43). In addition, we found that some NPY neurones are labelled by F-DAG. Thus, DAG could directly impact a fraction of NPY neurones that, in turn, represent a ghrelin target within the ARC (44). Unfortunately, we have been unable to test c-Fos induction in NPY neurones in the present study because these ARC cells cannot be visualised using conventional immunostaining in WT mice without colchicine treatment. A DAG-induced impairment of orexigenic effects of peripherally administered ghrelin via a direct action on ARC NPY neurones cannot be ruled out based on the observation that DAG increased c-Fos levels because this marker is not always associated with an increase in neuronal activity (45). Indeed, a potential cross-talk between DAG and ghrelin signalling pathways may take place at molecular levels downstream of c-Fos, particularly given the complexity of the intracellular mechanisms regulated by GHSR (46). By contrast, DAG can also inhibit the orexigenic effect of ghrelin by acting on a separated set of anorexigenic vmARC neurones. This possibility is supported by the finding that F-DAG labelled another unidentified type of ARC cells, and the observation that i.c.v. DAG and peripheral ghrelin treatment display an additive effect on c-Fos induction at the vmARC. Future studies testing whether the putative DAG receptor and GHSR are co-localised at the ARC are critical for discriminating between these possibilities. The induction of c-Fos has been previously used to identify the neuronal targets of DAG (33,47). Two independent studies have shown that DAG increases c-Fos in the POMC or nesfatin-1 neurones of the ARC. Interestingly, both DAG-responsive cell types maybe the same neuronal population because both peptides are co-produced in ARC neurones (48). In the present study, we confirmed that DAG activates POMC neurones. Notably, both DAG and ghrelin activated a similar percentage of ARC POMC neurones; however, DAG was more selective than ghrelin with respect to activating POMC neurones, at least based on the percentage of POMC neurones positive for c-Fos compared to the total number of neurones activated. Thus, it appears that DAG preferentially targets anorexigenic neurones within the ARC. Because POMC neurones are not labelled by F-DAG, the DAG-induced increase of c-Fos in POMC neurones is likely indirect. Although our data from the present study support the possibility that DAG and ghrelin differentially impact at the ARC level, it is interesting to highlight the observation that hypothalamic tanycytes display a significant uptake of i.c.v. F-DAG. Thus, it can be hypothesised that i.c.v. DAG may also inhibit the orexigenic effect of s.c. administered ghrelin by reducing the transport of the peripheral hormone to the hypothalamus. Future studies would be required to test these possibilities.

In summary, we provide the first direct evidence indicating that specific binding sites for DAG exist in the adult mouse hypothalamus. The localisation of a putative DAG receptor in the ARC neurones agrees with a potential role of DAG in food intake regulation.

Acknowledgements

This work was supported by PICT2011-2142 grant of the National Agency of Scientific and Technological Promotion of Argentina to MP. We would like to thank Dr Jeffrey Zigman for donating GHSR-null mice. GF, AC and MPC were supported by CONICET. The authors of the manuscript have no conflicts of interest to declare.

Received 25 June 2015,
revised 12 November 2015,
accepted 6 December 2015

References

1 Zizzari P, Hassouna R, Grouselle D, Epelbaum J, Tolle V. Physiological roles of preproghrelin-derived peptides in GH secretion and feeding. *Peptides* 2011; **32**: 2274–2282.
2 Hosoda H, Kojima M, Matsuo H, Kangawa K. Ghrelin and des-acyl ghrelin: two major forms of rat ghrelin peptide in gastrointestinal tissue. *Biochem Biophys Res Commun* 2000; **279**: 909–913.
3 De Vriese C, Gregoire F, Lema-Kisoka R, Waelbroeck M, Robberecht P, Delporte C. Ghrelin degradation by serum and tissue homogenates: identification of the cleavage sites. *Endocrinology* 2004; **145**: 4997–5005.
4 Hassouna R, Zizzari P, Tomasetto C, Veldhuis JD, Fiquet O, Labarthe A, Cognet J, Steyn F, Chen C, Epelbaum J, Tolle V. An early reduction in GH peak amplitude in preproghrelin-deficient male mice has a minor impact on linear growth. *Endocrinology* 2014; **155**: 3561–3571.
5 Howard AD, Feighner SD, Cully DF, Arena JP, Liberator PA, Rosenblum CI, Hamelin M, Hreniuk DL, Palyha OC, Anderson J, Paress PS, Diaz C, Chou M, Liu KK, McKee KK, Pong SS, Chaung LY, Elbrecht A, Dashkevicz M, Heavens R, Rigby M, Sirinathsinghji DJ, Dean DC, Melillo DG, Patchett AA, Nargund R, Griffin PR, DeMartino JA, Gupta SK, Schaeffer JM, Smith RG, Van der Ploeg LH. A receptor in pituitary and hypothalamus that functions in growth hormone release. *Science* 1996; **273**: 974–977.
6 Kojima M, Kangawa K. Ghrelin: structure and function. *Physiol Rev* 2005; **85**: 495–522.
7 Asakawa A, Inui A, Fujimiya M, Sakamaki R, Shinfuku N, Ueta Y, Meguid MM, Kasuga M. Stomach regulates energy balance via acylated ghrelin and desacyl ghrelin. *Gut* 2005; **54**: 18–24.
8 Inoue Y, Nakahara K, Maruyama K, Suzuki Y, Hayashi Y, Kangawa K, Murakami N. Central and peripheral des-acyl ghrelin regulates body temperature in rats. *Biochem Biophys Res Commun* 2013; **430**: 278–283.
9 Heppner KM, Piechowski CL, Muller A, Ottaway N, Sisley S, Smiley DL, Habegger KM, Pfluger PT, Dimarchi R, Biebermann H, Tschop MH, Sandoval DA, Perez-Tilve D. Both acyl and des-acyl ghrelin regulate adiposity and glucose metabolism via central nervous system ghrelin receptors. *Diabetes* 2014; **63**: 122–131.
10 Bednarek MA, Feighner SD, Pong SS, McKee KK, Hreniuk DL, Silva MV, Warren VA, Howard AD, Van Der Ploeg LH, Heck JV. Structure-function

© 2015 British Society for Neuroendocrinology

studies on the new growth hormone-releasing peptide, ghrelin: minimal sequence of ghrelin necessary for activation of growth hormone secretagogue receptor 1a. *J Med Chem* 2000; **43**: 4370–4376.
11 Callaghan B, Furness JB. Novel and conventional receptors for ghrelin, desacyl-ghrelin, and pharmacologically related compounds. *Pharmacol Rev* 2014; **66**: 984–1001.
12 Lear PV, Iglesias MJ, Feijoo-Bandin S, Rodriguez-Penas D, Mosquera-Leal A, Garcia-Rua V, Gualillo O, Ghe C, Arnoletti E, Muccioli G, Dieguez C, Gonzalez-Juanatey JR, Lago F. Des-acyl ghrelin has specific binding sites and different metabolic effects from ghrelin in cardiomyocytes. *Endocrinology* 2010; **151**: 3286–3298.
13 Togliatto G, Trombetta A, Dentelli P, Baragli A, Rosso A, Granata R, Ghigo D, Pegoraro L, Ghigo E, Brizzi MF. Unacylated ghrelin rescues endothelial progenitor cell function in individuals with type 2 diabetes. *Diabetes* 2010; **59**: 1016–1025.
14 Sato M, Nakahara K, Goto S, Kaiya H, Miyazato M, Date Y, Nakazato M, Kangawa K, Murakami N. Effects of ghrelin and des-acyl ghrelin on neurogenesis of the rat fetal spinal cord. *Biochem Biophys Res Commun* 2006; **350**: 598–603.
15 Perello M, Scott MM, Sakata I, Lee CE, Chuang JC, Osborne-Lawrence S, Rovinsky SA, Elmquist JK, Zigman JM. Functional implications of limited leptin receptor and ghrelin receptor coexpression in the brain. *J Comp Neurol* 2012; **520**: 281–294.
16 Cabral A, Suescun O, Zigman JM, Perello M. Ghrelin indirectly activates hypophysiotropic CRF neurons in rodents. *PLoS ONE* 2012; **7**: e31462.
17 Cabral A, Valdivia S, Fernandez G, Reynaldo M, Perello M. Divergent neuronal circuitries underlying acute orexigenic effects of peripheral or central ghrelin: critical role of brain accessibility. *J Neuroendocrinol* 2014; **26**: 542–554.
18 Akamizu T, Shinomiya T, Irako T, Fukunaga M, Nakai Y, Nakai Y, Kangawa K. Separate measurement of plasma levels of acylated and desacyl ghrelin in healthy subjects using a new direct ELISA assay. *J Clin Endocrinol Metab* 2005; **90**: 6–9.
19 Perello M, Stuart RC, Nillni EA. Differential effects of fasting and leptin on proopiomelanocortin peptides in the arcuate nucleus and in the nucleus of the solitary tract. *Am J Physiol Endocrinol Metab* 2007; **292**: E1348–E1357.
20 Paxinos G, Franklin KBJ. *The Mouse Brain in Stereotaxic Coordinates*. San Diego, CA: Academic Press, 2001.
21 Abercrombie M. Estimation of nuclear population from microtome sections. *Anatomical Record* 1946; **94**: 239–247.
22 Delhanty PJ, Sun Y, Visser JA, van Kerkwijk A, Huisman M, van Ijcken WF, Swagemakers S, Smith RG, Themmen AP, van der Lely AJ. Unacylated ghrelin rapidly modulates lipogenic and insulin signaling pathway gene expression in metabolically active tissues of GHSR deleted mice. *PLoS ONE* 2010; **5**: e11749.
23 Gropp E, Shanabrough M, Borok E, Xu AW, Janoschek R, Buch T, Plum L, Balthasar N, Hampel B, Waisman A, Barsh GS, Horvath TL, Bruning JC. Agouti-related peptide-expressing neurons are mandatory for feeding. *Nat Neurosci* 2005; **8**: 1289–1291.
24 Luquet S, Perez FA, Hnasko TS, Palmiter RD. NPY/AgRP neurons are essential for feeding in adult mice but can be ablated in neonates. *Science* 2005; **310**: 683–685.
25 Willesen MG, Kristensen P, Romer J. Co-localization of growth hormone secretagogue receptor and NPY mRNA in the arcuate nucleus of the rat. *Neuroendocrinology* 1999; **70**: 306–316.
26 Cabral A, Fernandez G, Perello M. Analysis of brain nuclei accessible to ghrelin present in the cerebrospinal fluid. *Neuroscience* 2013; **253**: 406–415.
27 Balland E, Dam J, Langlet F, Caron E, Steculorum S, Messina A, Rasika S, Falluel-Morel A, Anouar Y, Dehouck B, Trinquet E, Jockers R, Bouret SG, Prevot V. Hypothalamic tanycytes are an ERK-gated conduit for leptin into the brain. *Cell Metab* 2014; **19**: 293–301.
28 Banks WA, Tschop M, Robinson SM, Heiman ML. Extent and direction of ghrelin transport across the blood–brain barrier is determined by its unique primary structure. *J Pharmacol Exp Ther* 2002; **302**: 822–827.
29 Inhoff T, Wiedenmann B, Klapp BF, Monnikes H, Kobelt P. Is desacyl ghrelin a modulator of food intake? *Peptides* 2009; **30**: 991–994.
30 Chen C-Y, Inui A, Asakawa A, Fujino K, Kato I, Chen C-C, Ueno N, Fujimiya M. Des-acyl ghrelin acts by CRF Type 2 receptors to disrupt fasted stomach motility in conscious rats. *Gastroenterology* 2005; **129**: 8–25.
31 Uchida A, Zigman JM, Perello M. Ghrelin and eating behavior: evidence and insights from genetically-modified mouse models. *Front Neurosci* 2013; **7**: 121.
32 Neary NM, Druce MR, Small CJ, Bloom SR. Acylated ghrelin stimulates food intake in the fed and fasted states but desacylated ghrelin has no effect. *Gut* 2006; **55**: 135.
33 Inhoff T, Monnikes H, Noetzel S, Stengel A, Goebel M, Dinh QT, Riedl A, Bannert N, Wisser AS, Wiedenmann B, Klapp BF, Tache Y, Kobelt P. Desacyl ghrelin inhibits the orexigenic effect of peripherally injected ghrelin in rats. *Peptides* 2008; **29**: 2159–2168.
34 Toshinai K, Yamaguchi H, Sun Y, Smith RG, Yamanaka A, Sakurai T, Date Y, Mondal MS, Shimbara T, Kawagoe T, Murakami N, Miyazato M, Kangawa K, Nakazato M. Des-acyl ghrelin induces food intake by a mechanism independent of the growth hormone secretagogue receptor. *Endocrinology* 2006; **147**: 2306–2314.
35 Matsuda K, Miura T, Kaiya H, Maruyama K, Shimakura S, Uchiyama M, Kangawa K, Shioda S. Regulation of food intake by acyl and des-acyl ghrelins in the goldfish. *Peptides* 2006; **27**: 2321–2325.
36 Sato T, Fukue Y, Teranishi H, Yoshida Y, Kojima M. Molecular forms of hypothalamic ghrelin and its regulation by fasting and 2-deoxy-d-glucose administration. *Endocrinology* 2005; **146**: 2510–2516.
37 Furness JB, Hunne B, Matsuda N, Yin L, Russo D, Kato I, Fujimiya M, Patterson M, McLeod J, Andrews ZB, Bron R. Investigation of the presence of ghrelin in the central nervous system of the rat and mouse. *Neuroscience* 2011; **193**: 1–9.
38 Murakami N, Hayashida T, Kuroiwa T, Nakahara K, Ida T, Mondal MS, Nakazato M, Kojima M, Kangawa K. Role for central ghrelin in food intake and secretion profile of stomach ghrelin in rats. *J Endocrinol* 2002; **174**: 283–288.
39 Theander-Carrillo C, Wiedmer P, Cettour-Rose P, Nogueiras R, Perez-Tilve D, Pfluger P, Castaneda TR, Muzzin P, Schurmann A, Szanto I, Tschop MH, Rohner-Jeanrenaud F. Ghrelin action in the brain controls adipocyte metabolism. *J Clin Investig* 2006; **116**: 1983–1993.
40 Wang Q, Liu C, Uchida A, Chuang JC, Walker A, Liu T, Osborne-Lawrence S, Mason BL, Mosher C, Berglund ED, Elmquist JK, Zigman JM. Arcuate AgRP neurons mediate orexigenic and glucoregulatory actions of ghrelin. *Mol Metab* 2014; **3**: 64–72.
41 Nakazato M, Murakami N, Date Y, Kojima M, Matsuo H, Kangawa K, Matsukura S. A role for ghrelin in the central regulation of feeding. *Nature* 2001; **409**: 194–198.
42 Chen HY, Trumbauer ME, Chen AS, Weingarth DT, Adams JR, Frazier EG, Shen Z, Marsh DJ, Feighner SD, Guan XM, Ye Z, Nargund RP, Smith RG, Van der Ploeg LH, Howard AD, MacNeil DJ, Qian S. Orexigenic action of peripheral ghrelin is mediated by neuropeptide Y and agouti-related protein. *Endocrinology* 2004; **145**: 2607–2612.
43 Elias CF, Saper CB, Maratos-Flier E, Tritos NA, Lee C, Kelly J, Tatro JB, Hoffman GE, Ollmann MM, Barsh GS, Sakurai T, Yanagisawa M, Elmquist JK. Chemically defined projections linking the mediobasal hypothalamus and the lateral hypothalamic area. *J Comp Neurol* 1998; **402**: 442–459.
44 Wang L, Saint-Pierre DH, Tache Y. Peripheral ghrelin selectively increases Fos expression in neuropeptide Y - synthesizing neurons in mouse hypothalamic arcuate nucleus. *Neurosci Lett* 2002; **325**: 47–51.

© 2015 British Society for Neuroendocrinology

45 Hoffman GE, Lyo D. Anatomical markers of activity in neuroendocrine systems: are we all 'fos-ed out'? *J Neuroendocrinol* 2002; **14**: 259–268.
46 Lopez Soto EJ, Agosti F, Cabral A, Mustafa ER, Damonte VM, Gandini MA, Rodriguez S, Castrogiovanni D, Felix R, Perello M, Raingo J. Constitutive and ghrelin-dependent GHSR1a activation impairs CaV2.1 and CaV2.2 currents in hypothalamic neurons. *J Gen Physiol* 2015; **146**: 205–219.
47 Stevanovic DM, Grefhorst A, Themmen AP, Popovic V, Holstege J, Haasdijk E, Trajkovic V, van der Lely AJ, Delhanty PJ. Unacylated ghrelin suppresses ghrelin-induced neuronal activity in the hypothalamus and brainstem of male rats. *PLoS ONE* 2014; **9**: e98180.
48 Brailoiu GC, Dun SL, Brailoiu E, Inan S, Yang J, Chang JK, Dun NJ. Nesfatin-1: distribution and interaction with a G protein-coupled receptor in the rat brain. *Endocrinology* 2007; **148**: 5088–5094.

© 2015 British Society for Neuroendocrinology